VENTED HYDROGEN DEFLAGRATIONS IN CONTAINERS: EFFECT OF CONGESTION FOR HOMOGENEOUS MIXTURES

Skjold, T., Hisken, H., Lakshmipathy, S., Atanga, G., van Wingerden, M., Olsen, K.L., Holme, M.N., Turøy, N.M., Mykleby, M. and van Wingerden, K.

Gexcon, Fantoftvegen 38, 5072 Bergen, Norway, trygve@gexcon.com

ABSTRACT

This paper presents results from an experimental study of vented hydrogen deflagrations in 20-foot ISO containers. The scenarios investigated include 14 tests with explosion venting through the doors of the containers, and 20 tests with venting through openings in the roof. The parameters investigated include hydrogen concentration, vent area, type of venting device, and the level of congestion inside the containers. All tests involved homogeneous and initially quiescent hydrogen-air mixtures. The results demonstrate the strong effect of congestion on the maximum reduced explosion pressures, which typically is not accounted for in current standards and guidelines for explosion protection. The work is a deliverable from work package 2 (WP2) in the project "Improving hydrogen safety for energy applications through pre-normative research on vented deflagrations", or HySEA (www.hysea.eu), which receives funding from the Fuel Cells and Hydrogen Joint Undertaking (FCH JU) under grant agreement no. 671461.

1 INTRODUCTION

1.1 The HySEA project

Fires and explosions represent a significant hazard for hydrogen installations, and specific measures are generally required for reducing the risk to a tolerable level [1]. It is common practice in industry to install electrolysers, refuelling stations, fuel cell backup systems and other equipment for hydrogen energy applications in containers or smaller enclosures.

Explosion venting is a frequently used measure for reducing the consequences of hydrogen deflagrations in confined systems. Whereas most enclosures used for hydrogen applications in industry are inherently congested, the empirical correlations for the design of venting devices found in international standards, such as EN 14994 [2] and NFPS 68 [3], originate from explosion experiments performed with empty vessels. This situation motivated the Fuel Cells and Hydrogen Joint Undertaking (FCH JU) call for proposal FCH-04.3-2014: *Pre-normative research on vented deflagrations in containers and enclosures for hydrogen energy applications*. In 2015, FCH JU granted funding to the project *Improving Hydrogen Safety for Energy Applications through pre-normative research on vented deflagrations*, or HySEA (www.hysea.eu). The HySEA project started in September 2015. The members of the HySEA consortium are Gexcon (coordinator), University of Warwick (UWAR), University of Pisa (UNIPI), Fike Europe, Impetus Afea and Hefei University of Technology (HFUT). The work in the HySEA project is organized in five work packages (WPs):

- WP1: Engineering models and standards
- WP2: Experimental campaigns in containers and smaller enclosures
- WP3: Advanced modelling: computational fluid dynamics (CFD) and finite element (FE) analysis
- WP4: Exploitation, dissemination and communication
- WP5: Project management

The research activities in WP2 include two experimental studies: UNIPI investigates hydrogen explosions in smaller enclosures, and Gexcon conducts full-scale explosion experiments in 20-foot ISO containers. Each study consists of two separate campaigns: explosions in initially quiescent and homogeneous gas clouds, and explosions in initially turbulent and/or inhomogeneous clouds. In addition, HFUT conducts experiments at laboratory scale and in 40-foot ISO containers.

This paper presents the results from the first of the two experimental campaigns that Gexcon conducted as part of the HySEA project: vented deflagration tests with homogeneous mixtures in 20-foot containers. The output from WP2 is important input to WP1, where the aim is to develop and validate engineering models suitable for standards, as well as to the work on CFD and FE methods in WP3.

1.2 Previous work

Vented hydrogen deflagrations have been extensively studied in the past, but primarily in empty enclosures. The experiments conducted by Sommersel *et al.* in a 20-foot ISO container [4-5], with varying degrees of congestion, resembles the work presented here. However, these experiments involved ignition of transient releases, and is therefore more relevant for the second experimental campaign in the HySEA project, which will focus on scenarios with initial turbulence and inhomogeneous gas clouds.

2 EXPERIMENTS

The experimental campaign with homogeneous mixtures included 34 experiments: tests 1-14 with venting through the container doors, and tests 15-34 with vent openings in the roof [6-7]. Gexcon performed the experiments at the remote test site on the island of Sotra outside Bergen during the period September 2016 to January 2017. Figure 1 shows the test site with a container ready for testing.

Figure 1: The test site at Sotra with a 20-foot container prepared for testing.

The experimental setup consisted of standard 20-foot ISO containers, fitted with a steel frame for instrumentation and obstacle support. In tests 15-34, another steel frame was fitted to the roof of the containers for mounting vent covers. Gexcon obtained 12 containers from the same manufacturing series for the two experimental campaigns in the HySEA project, and used five containers in the first campaign. Figure 2 shows one of the containers, before and after testing. The inner dimensions of the containers were 5.87 m × 2.35 m × 2.40 m, i.e. a total volume of about 33 m^2.

Figure 2: A 20-foot container before (left) and after (right) testing.

Figure 3 shows the steel frame used to protected the internal pressure transducers (P01-P08) and signal cables, and to support the obstacles. The frame was constructed from 200 mm × 75 mm U-beams (UNP).

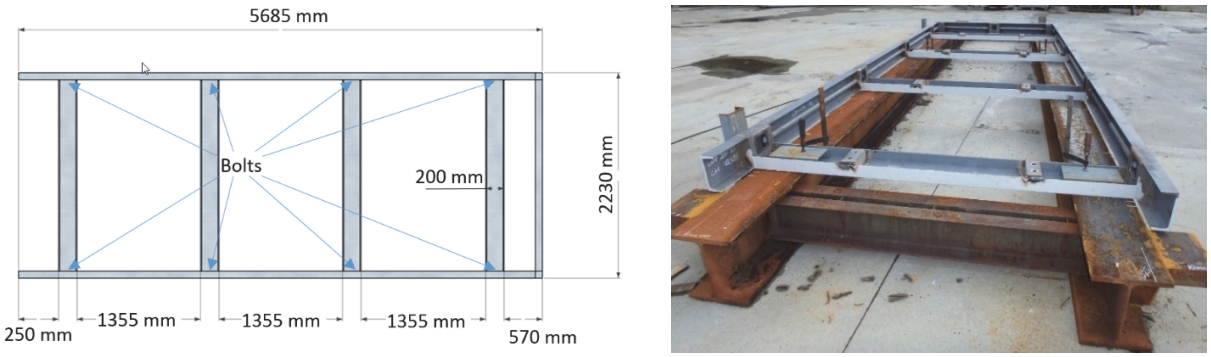

Figure 3. Dimensions of steel frame (left) and steel frame positioned on foundation (right).

Figures 4 and 5 show the two obstacles: a basket with 20 high-pressure gas bottles, 50-litre each and 5 mm spacing between the bottles, and a pipe rack with four layers of pipes.

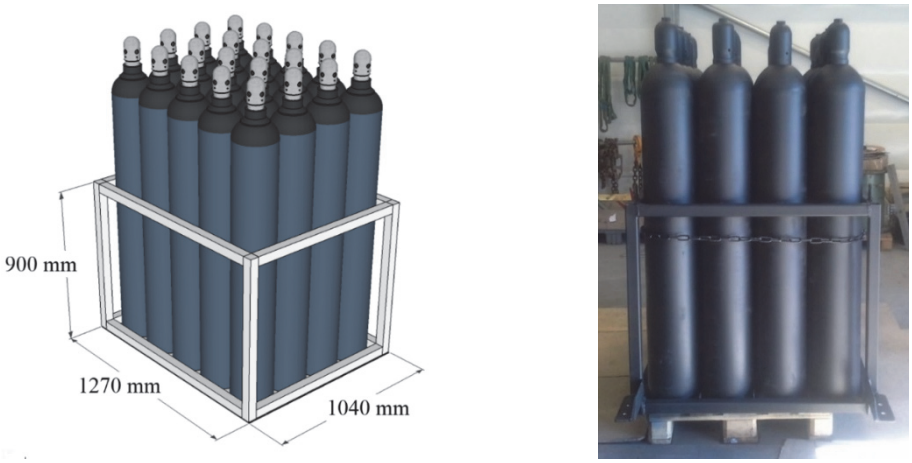

Figure 4. Dimensions of bottle basket (left) and basket with 50-litre high-pressure cylinders (right).

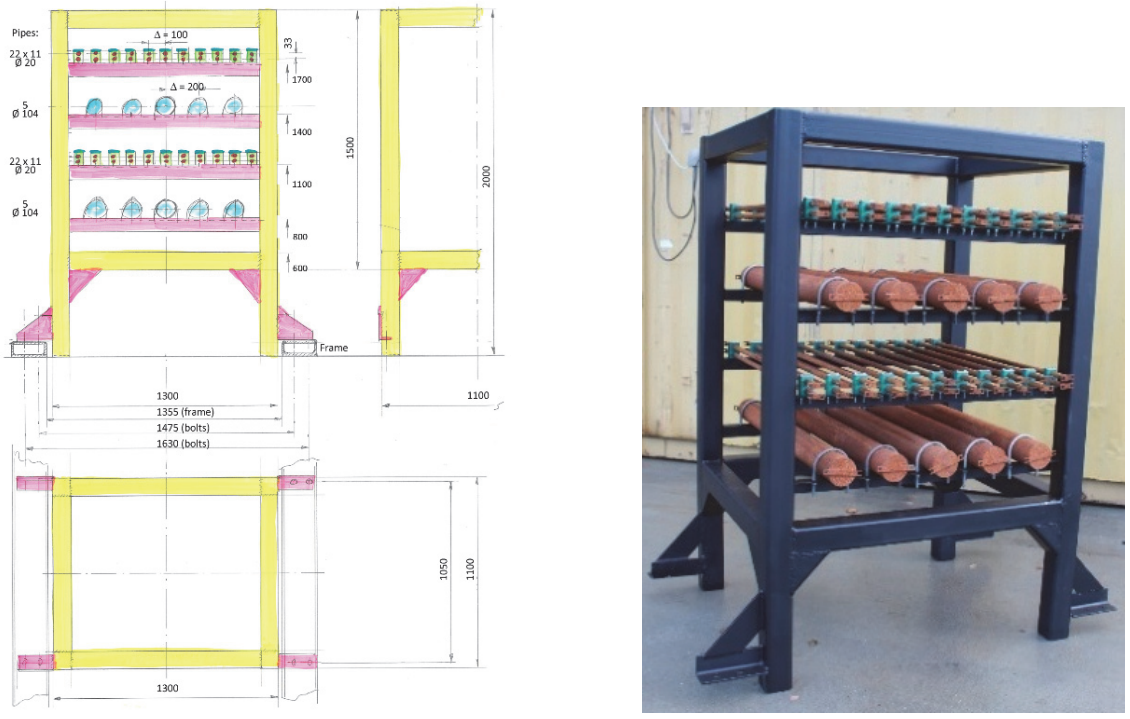

Figure 5. Dimensions of pipe rack (left) and pipe rack obstacle (right).

A recirculation system was used to prepare homogeneous hydrogen-air mixtures in the containers. To eliminate the effect of initial turbulence, the explosive atmosphere inside the container was isolated from the recirculation system by closing remotely operated valves several minutes prior to ignition. A Servomex Xendos 2223 oxygen analyser measured the gas concentrations in the recirculation system and at selected points inside the container to the moment of ignition with. The ignition source was an electric inductive spark (1 mJ), triggered at a specific time. For tests with venting through the door, the spark plug was located at the back wall of the container at mid-height (position A), and for tests with venting through the roof it was located at the centre of the floor (position B).

Figure 6 illustrates the position of the pressure and displacement sensors. Eight Kistler 701A/7031 piezoelectric pressure sensors with Kistler 5073A211 charge amplifiers measured the internal pressures P01-P08 inside the container, and three Kistler 4043A piezoresistive pressure gauges with Kistler 4601 amplifiers measured the far-field blast pressures P09-P11. The internal sensors were positioned at the U-beams along the side walls of the container, in the same position as the eight bolts fixing the frame to a solid foundation underneath the container, 85 mm from the side wall, and 200 mm above the floor.

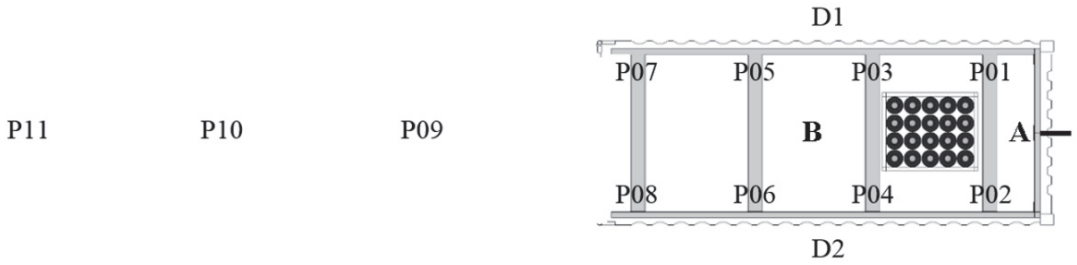

Figure 6: Positions for pressure (P01-P11) and deflection (D1-D2) sensors, and ignition source (A/B).

Figure 1 shows the holders for the three external pressure sensors P09-P11, located 5 m, 10 m and 15 m from the door on the container, and about 1.65 m above ground. The sensors were mounted on skimmer plates oriented perpendicular to the blast front, measuring side-on pressures. For tests with venting through the roof, P10 was moved to a position 2.7 m above the roof of the container, and 1.25 m from the back wall (inclined tube shown in Figure 1).

Two Acuity AR700-50 Laser displacement sensors (D1-D2) measured the dynamic deflection of the container walls. The lasers were operated at around 10 kHz, and measured the displacement of the container wall at the centre of the side walls. The explosion events were recorded with two Edgertronic SC1 high-speed cameras and one regular JVC GZ-RX515BE video camera. Four NI-9215 (BNC) C series voltage input modules from National Instruments recorded the signals from the pressure and deflection sensors at a sampling frequency of 100 kHz. The results from the first tests revealed significant challenges with noise and drift for the pressure measurements. The noise was gradually reduced by replacing signal cables and modifying other parts of the measurement system.

The recorded data were smoothed with the digital filter technique proposed by Savitzky and Golay [8]. Oscillations associated with alternating current at the frequency (50 Hz) of the mains electricity were processed with a digital filter, and the filtered data were used for data series where visual inspection of the plotted data and a frequency spectrum generated by fast Fourier transform (FFT) showed that the filtering had the desired effect. The problems associated with noise were most severe for the weakest explosions, but several data series were significantly influenced by drift in the pressure signals. Some of these issues could be mitigated by replacing signal cables for sensors P03-P08, i.e. the longest cables between the piezoelectric sensors and the charge amplifiers.

Figure 7 shows vertical cross-sections of experimental configurations: each of the two obstacles, i.e. the bottle basket (B) and the pipe rack (P), could be fixed in inner (1), centre (2) or outer (3) position on the frame, and the ignition source (spark) could be located at the centre of the back wall (A) or at the centre of the floor (B). It was possible to install one obstacle in the inner position (e.g. P1) and the other in the outer position (e.g. B3), denoted ‘P1B3’ for test 14 with venting through the door in Figure 6. Table 1 summarizes the experimental conditions for the 14 tests with venting through the container doors and Table 2 summarizes the conditions for the 20 tests with venting through the roof.

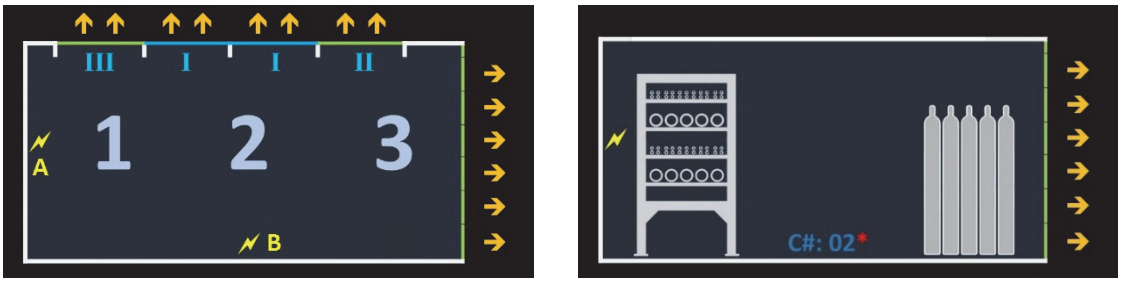

Figure 7. Obstacle, ignition and vent locations (left) and example of configuration for test 14 (right).

Table 1: Summary of the experiments with venting through the container doors.

Configuration	Test	A_v (m^2)	[H_2] (vol.%)	Ign. pos.	$P_{red, max}$ (bar)
Frame only (FO), doors open (O)	01	5.64	15	A	0.040
	02	5.64	15	A	0.047
	05	5.64	15	A	0.039
Bottle basket (B1), doors open (O)	03	5.64	15	A	0.077
	04	5.64	15	A	0.064
	06	5.64	15	A	0.045
	10	5.64	18	A	0.130
	07	5.64	21	A	0.190
	08	5.64	24	A	0.390
Bottle basket (B1), doors closed (C)	09*	0.00	24	A	1.447
Pipe rack (P1), doors open (O)	11	5.64	15	A	0.050
	12	5.64	18	A	0.120
	13	5.64	21	A	0.279
Pipe rack and bottle basket (P1 B3), doors open (O)	14*	5.64	21	A	0.939

Table 2: Summary of experiments with venting through the container roof.

Configuration	Test	A_v (m^2)	[H_2] (vol.%)	Ign. pos.	$P_{red, max}$ (bar)
Frame only (FO), perforated plastic film (O)	25	4.0	21	B	0.146
	21	6.0	21	B	0.120
	16	8.0	21	B	0.190
Pipe rack (P2), perforated plastic film (O)	24	4.0	21	B	0.150
	22	6.0	21	B	0.142
	17	8.0	21	B	0.124
Pipe rack (P2), perforated plastic film (O)	34*	8.0	42	B	1.076
Pipe rack (P2), perforated plastic film (O)	29	4.0	24	B	0.414
	23	6.0	24	B	0.168
	19	8.0	24	B	0.136
Frame only (FO), commercial vent panels (P)	32	4.0	21	B	0.214
	26	6.0	21	B	0.245
	15	8.0	21	B	0.191
Pipe rack (P2), commercial vent panels (P)	33	4.0	21	B	0.261
	27	6.0	21	B	0.301
	31	6.0	21	B	0.249
	18	8.0	21	B	0.234
	30	8.0	21	B	0.214
Pipe rack (P2), commercial vent panels (P)	28*	6.0	24	B	0.45 / 0.73 ?
	20*	8.0	24	B	0.334

The eight openings in the roof could be sealed with plastic film (0.2 mm 99 % polyethylene, specific weight 0.185 kg m^{-2}), perforated along the edges, or with commercial vent panels from Fike (vent area A_v = 1 m^2 per panel, static opening pressure P_{stat} = 0.10 bar, weight 6.8 kg m^{-2}). Blind flanges were used to close up to four of the eight openings, allowing for vent areas of 4.0, 6.0 or 8.0 m^2. Except from test 34, the experiments focused on hydrogen concentrations [H_2] in the range 15-24 vol.%. The first campaign consumed five containers, and the last test with each container is marked (*) in tables 1 and 2. The fact that the same container was used in several tests influences the repeatability of the experiments, especially with respect to the measurements of structural response.

3 RESULTS

3.1 Venting through the container doors

Figure 8 summarizes the results from the tests with explosion venting through the doors. The highest pressures were measured in the closed end of the container (P01 & P02), and the external pressures, i.e. the side-on pressures measured with pressure transducers mounted on skimmer plates, located 5, 10 and 15 m from the vent opening (i.e. the door plane), decay consistently with increasing distance from the container. In test 09, with the doors closed, the container ruptured at the back wall, and both doors were thrown a considerable distance (up to about 30 m). The back wall of the container ruptured in test 14 as well, which is the only test with both obstacles installed inside the container (ref. figures 7 and 10).

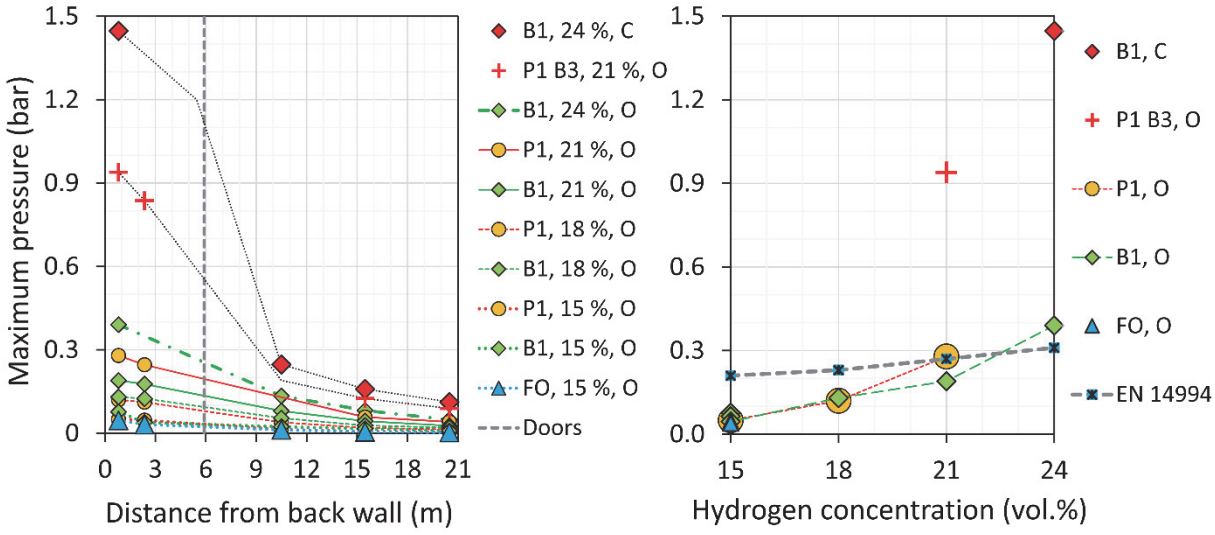

Figure 8. Maximum pressure vs. distance (left) and hydrogen concentration (right) for tests 1-14.

Figure 9 shows selected pressure-time histories from the tests with venting through the container doors. The maximum pressure, or maximum reduced explosion pressure $P_{red,max}$, increases consistently with increasing fuel concentration for both obstacle configurations (B1 and P1). At the same time, the shape of the pressure-time curves changes from two distinct peaks for the 15 vol.% mixtures towards one single peak for the 21 and 24 vol.% mixtures. The maximum pressures measured outside the container (indicated by stars) occur shortly after the secondary peaks, where acoustic oscillations enhance the rate of combustion as the flame approaches the walls of the container.

The vertical dotted line in the plot for test 9 indicates the time when the container doors started to open – this occurred when the internal pressure was about 1.1-1.3 barg. Although the shapes of the pressure-time curves differ somewhat for the bottle basket obstacle relative to the pipe rack obstacle, the maximum pressures are similar for the 15 and 18 vol.% mixtures. However, there is a clear tendency towards higher pressures for the pipe rack obstacle for the more reactive mixtures.

Figure 10 compares the results from test 13 (P1) and 14 (P1 B3), for 21 vol.% hydrogen in air. The significant increase in pressure for test 14 demonstrates the effect of reducing the effective vent area by adding the bottle basket obstacle close to the vent opening.

Figure 11 shows the repeatability of tests with venting through the doors. The measurement of low explosion pressures, in the range 40-80 mbar, required high degree of amplification, and resulted in poor signal-to-noise ratio. Some of the pressure measurements are also significantly influenced by drift. The maximum explosion pressures are nevertheless reasonably consistent. The displacement measurements show significant scatter, especially after the initial implement corresponding to the main pressure peak.

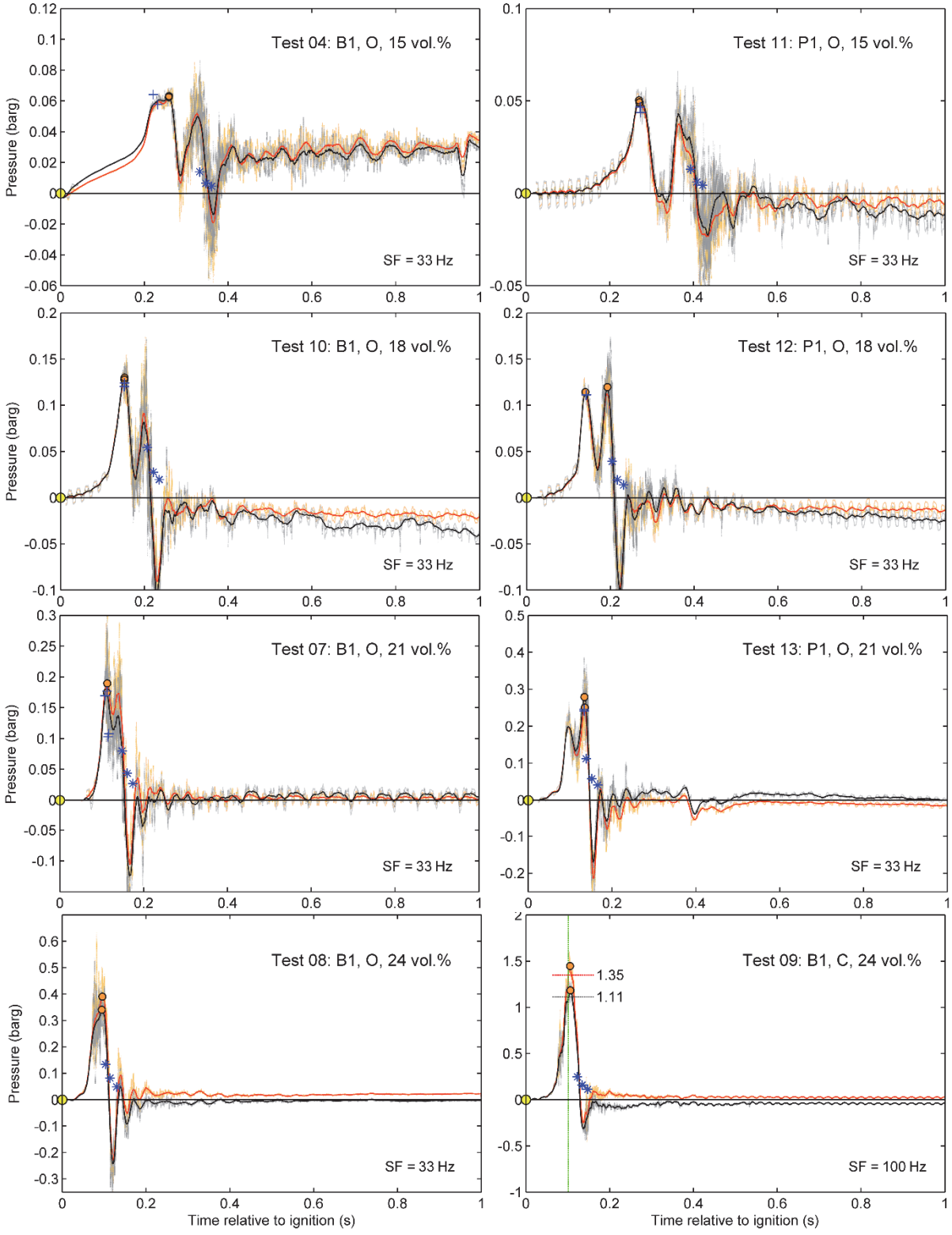

Figure 9. Pressure-time histories (P01 & P02) for selected tests with venting through the doors.

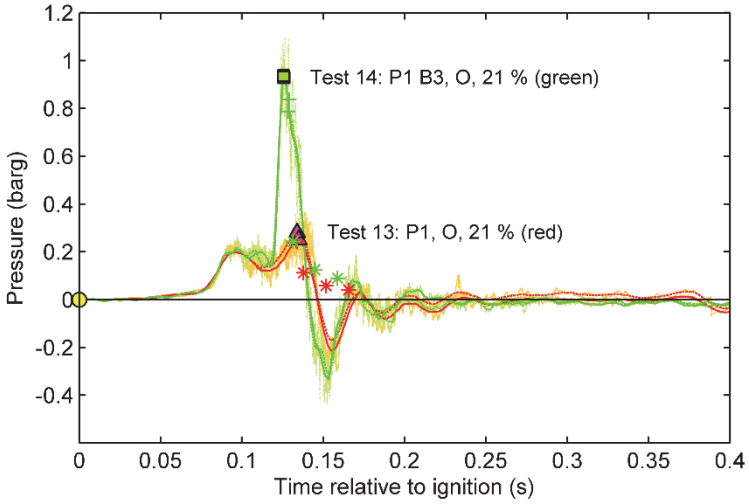

Figure 10. Pressure-time histories (P01 & P02) for tests 13 and 14.

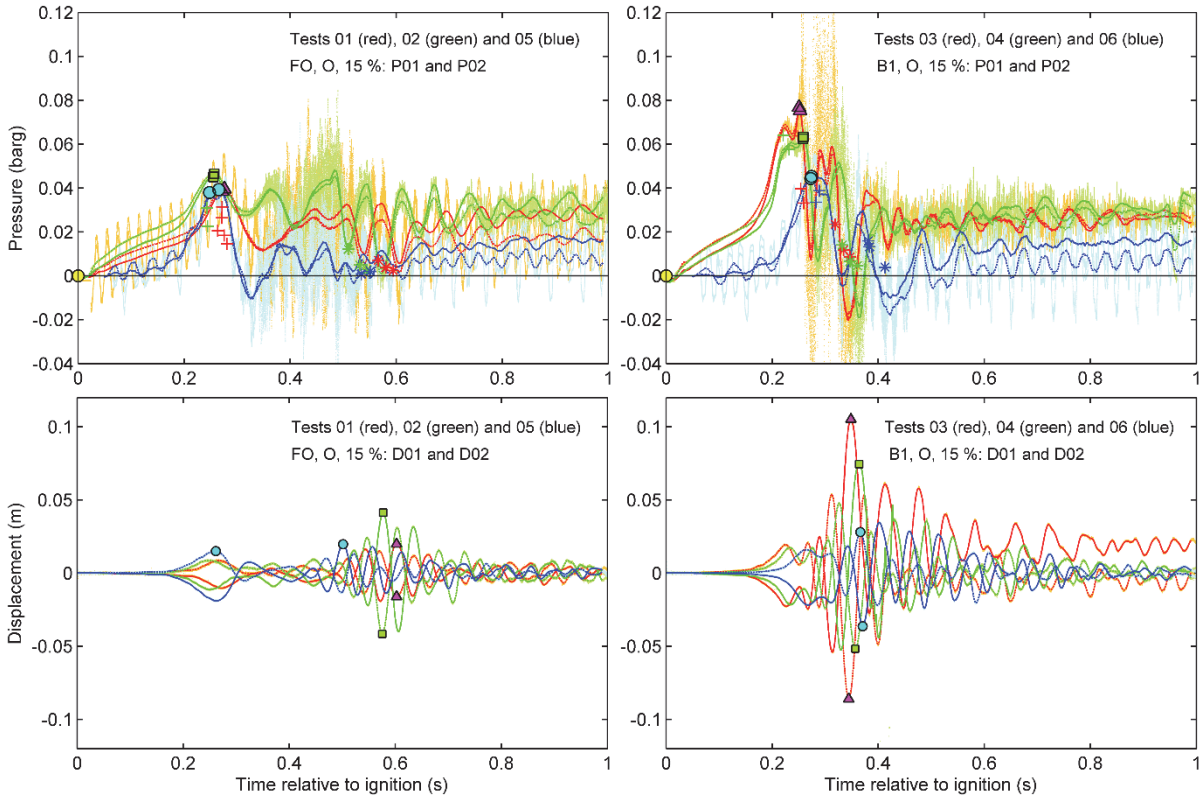

Figure 11. Pressure and deflection for repeated tests with venting through the doors.

3.2 Venting through the roof of the containers

Figure 12 summarizes the results for the tests with venting through the roof. Tests with vent panels show consistently higher pressures compared to tests with perforated plastic film, for otherwise identical conditions. The effect of increasing the vent area is most pronounced for the more reactive mixtures.

The containers were severely deformed in tests 20 and 28 (P2, 24 %, P). Figure 13 illustrates that the uncertainty ('?') in the maximum pressure for test 28 is due to a deviating pressure signal from sensor P06, relative to the seven other sensors inside the container. Since the pressure returns to a reasonable level after about 0.2 s, it is not straightforward to dismiss the deviating result for P06. However, using the higher value in the analysis has severe implications for the overall results in Figure 12.

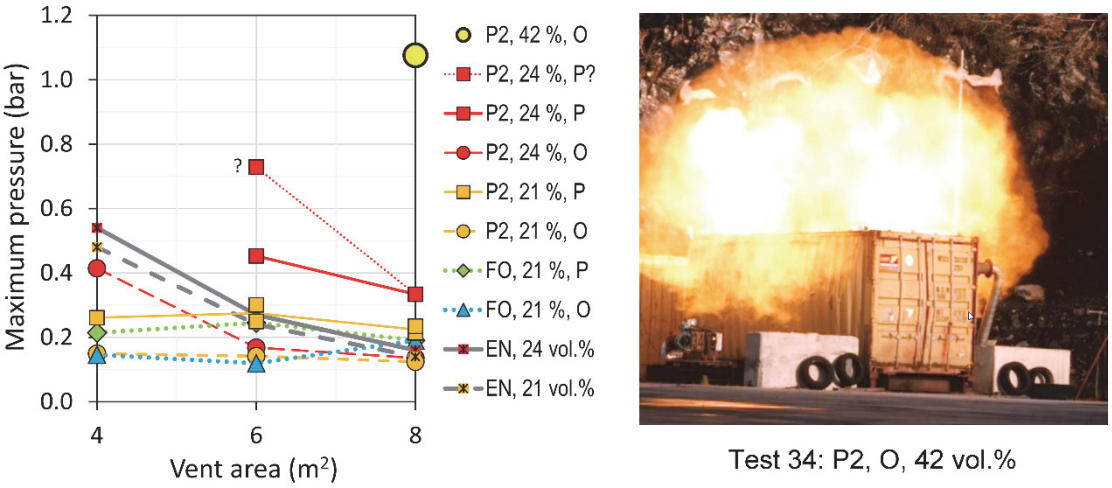

Figure 12. Maximum pressure vs. vent area for tests 15-34 (left) and vented explosion (right).

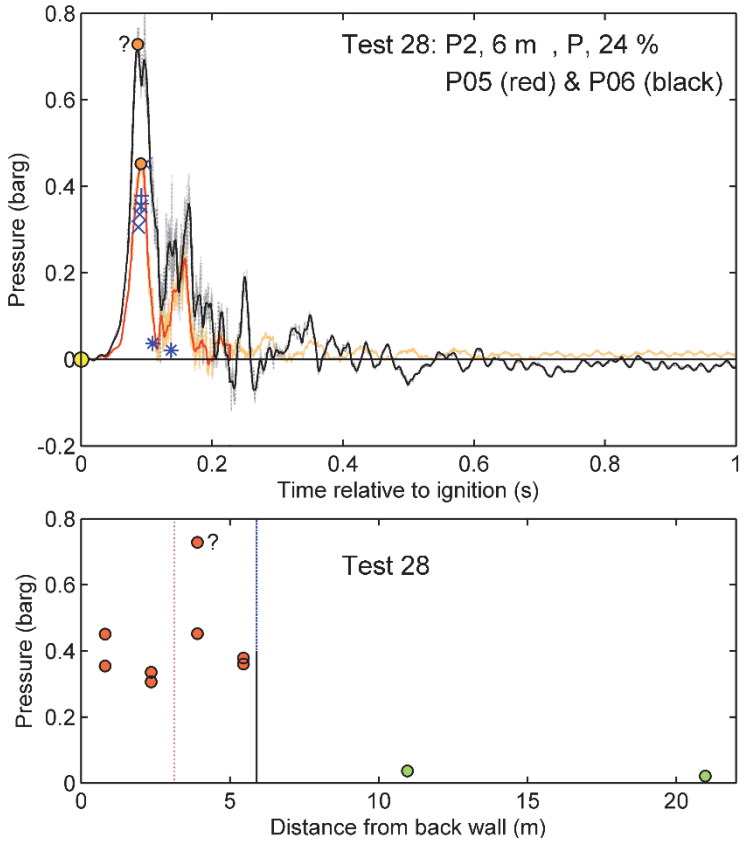

Figure 13. Pressure-time histories for test 28 (above) and variation in pressure with distance (below).

Figure 14 shows selected pressure-time histories from the tests with venting through the roof of the container. Smaller vent areas result in more pronounced secondary peaks, typically accompanied by high-frequency oscillating behaviour. Enhanced rate of combustion in the remaining fuel due to acoustic instabilities is a plausible explanation for the secondary peaks. The increased time from ignition to reaching the maximum pressure, for decreasing vent area in tests 33, 31 and 18 with commercial panels, can be a result of inherent variability between tests. Figure 15 demonstrates that the time for onset of significant pressure increase can vary significantly in these tests.

The effect of increasing vent area is most pronounced for the more reactive mixtures. The results for test 34 display a secondary peak with significant amplitude and duration, and without obvious signs of the oscillating pressure fluctuations that usually accompany combustion processes couples with acoustic instabilities. It is likely that the external explosion blocks the outflow from the container, and that rapid afterburning of remaining fuel produces the strong secondary peak.

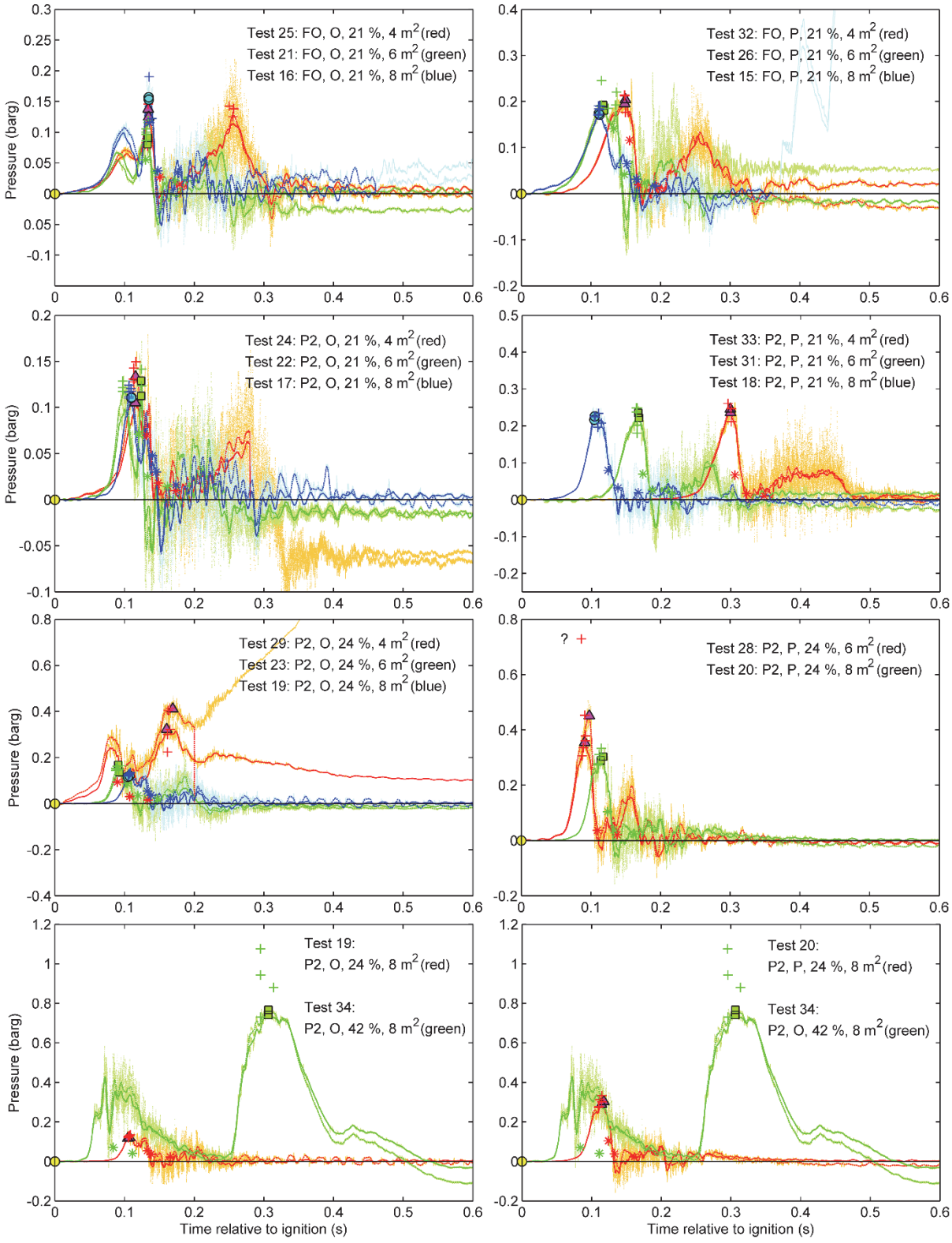

Figure 14. Pressure-time histories (P01 & P02) for selected tests with venting through the roof.

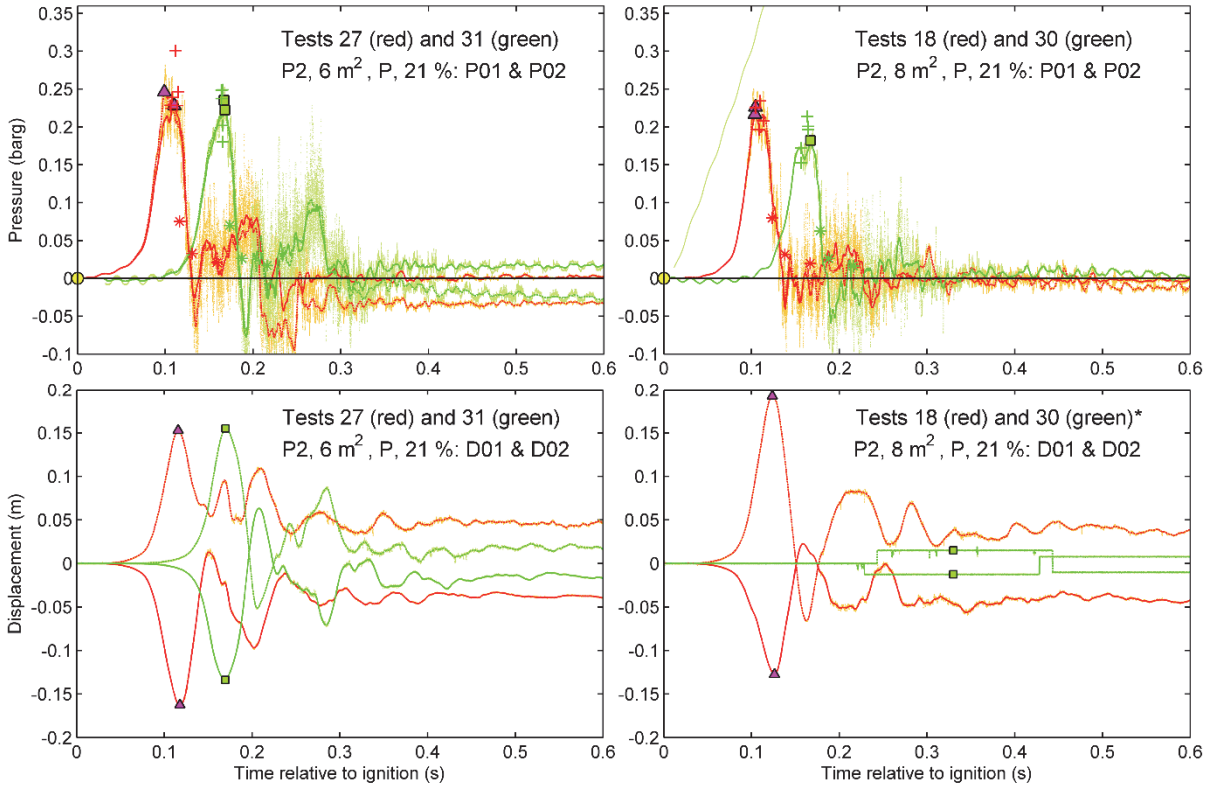

Figure 15. Pressure and deflection for repeated tests with venting through the roof.

Figure 5 shows selected frames from some of the tests: doors opening in test 09, venting through the doors in test 14, and opening of vent panels on the roof in test 18. The vent panel opened simultaneously in all tests with commercial panels. The main structure of the container remained intact in all tests, except from test 09 where the hinges broke as the doors opened, and the doors were thrown a considerable distance (up to about 30 m). This highlights the importance of securing attached structural elements, such as doors, louvers, ventilators, etc.

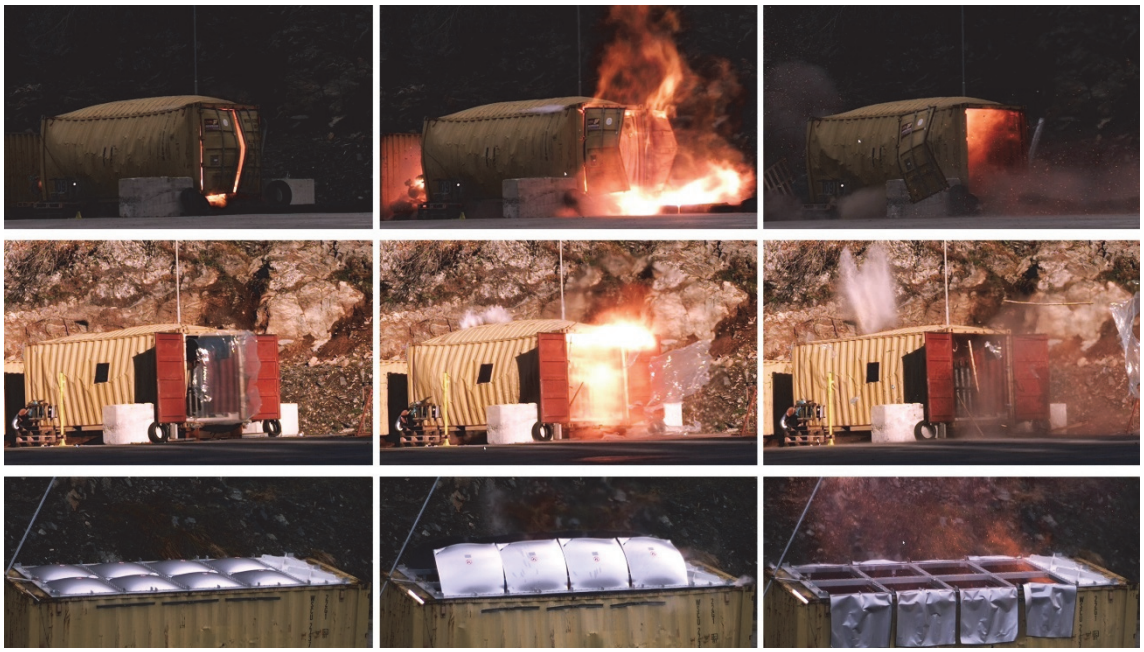

Figure 16. Selected frames from test 09 (top), test 14 (middle) and test 18 (bottom).

4 DISCUSSION

An experimental campaign with homogeneous and initially quiescent hydrogen-air mixtures, ignited to deflagration in vented 20-foot ISO containers, has produced a valuable set of data that can be used for validating engineering models and CFD tools. Most of the 34 experiments included measurements of the structural response of the container walls, and these results are suitable for validating FE models, including the coupling between CFD and FE tools. The range of experimental conditions that could be investigated was somewhat limited, partly due to the available budget, and partly because of the limited strength of the ISO containers.

Figures 8 and 12 include over-pressure predictions obtained with the European standard EN 14994 [2]. The empirical correlation in this standard is only valid for empty enclosures and flammable atmospheres with gas explosion constant $K_G \leq 550$ bar m s^{-1} (i.e. mixtures with less than about 26 % hydrogen in air). These estimates involve the use of published K_G values for the relevant hydrogen concentrations [9], which implies significant uncertainty since flame wrinkling and other instabilities cause the experimentally determined K_G values to vary significantly with the volume and shape of the test vessel. Furthermore, since the EN standard assumes a static opening pressure P_{stat} of 0.10 bar, the correlation over-predicts $P_{red,\,max}$ for tests with low reactivity and vent openings covered by plastic film. The effect of internal congestion on $P_{red,\,max}$ increases for the more reactive fuel-air mixtures, and the standard significantly under-predicts the explosion pressure for tests with internal congestion and 24 vol.% hydrogen in air. This demonstrates the need for updated engineering models that can account for the effect of congestion and/or initial turbulence.

Test 09, with the container doors closed, serves as a reminder of the hazard posed by projectiles: one door bounced off the gravel on the side of the container, hit the hillside some 10 m above ground, and landed about 30 m from the container. The container ruptured at an internal overpressure of about 1.1-1.3 bar. Test 14, with both obstacles installed inside the container (P1 B3), demonstrates the strong effect internal congestion can have on vented explosions. The reason for the high over-pressures observed in this test is presumably a combination of flame acceleration through the pipe rack (P1) and the blocking effect of the bottle basket located near the vent opening (B3).

The significant increase in explosion pressure from tests 23 and 19 (i.e. P2, 24 vol.%, O) to tests 28 and 20 (i.e. P2, 24 vol.%, P), for A_v = 6.0 and 8.0 m^2 in Figure 15, suggests that vent panels with lower opening pressure and/or lower mass can provide more effective protection of relatively weak structures, such as shipping containers. The results obtained for test 34, with 42 vol.% hydrogen, demonstrate that explosion venting in principle can protect a 20-foot ISO container under near worst-case conditions, provided deflagration-to-detonation-transition (DDT) does not occur. However, this test also demonstrates the inherent limitations to the level of protection that can be achieved for explosions involving more reactive mixtures. Initial turbulence produced by forced ventilation, or the leak itself, may increase the rate of combustion, and hence the maximum pressure in vented explosions.

5 CONCLUSIONS AND FURTHER WORK

The first part of the experimental study of vented hydrogen deflagrations in 20-foot ISO containers in the HySEA project produced valuable validation data for modellers [6]. The results demonstrate the strong effect of congestion on vented deflagrations, especially for the more reactive mixtures. The results also highlight the importance of considering projectiles, such as the container doors, in risk assessments. The verification and validation of CFD and FE models in the HySEA project entail direct comparison between experimental results and model predictions. It is foreseen that this process will result in improved understanding of the physical and chemical phenomena involved in vented hydrogen deflagrations. The next experimental campaign in 20-foot containers will focus on deflagrations in inhomogeneous mixtures, resulting from more realistic releases, with or without initial turbulence in the enclosure. The experimental results from the HySEA project are particularly well suited for testing and validating engineering models for vented hydrogen deflagrations, and hence for improving the empirical correlations for design of venting devices in international standards.

ACKNOWLEDGEMENTS

The HySEA project receives funding from the Fuel Cells and Hydrogen 2 Joint Undertaking under grant agreement No. 671461. This Joint Undertaking receives support from the European Union's Horizon 2020 research and innovation programme and United Kingdom, Italy, Belgium and Norway.

REFERENCES

1 Skjold, T., Siccama, D., Hisken, H., Brambilla, A, Middha, P., Groth, K.M. & LaFleur, A.C., 3D risk management for hydrogen installations, *International Journal of Hydrogen Energy*, **42**, 2017, pp. 7721-7730.

2 EN 14994, *Gas explosion venting protective systems*, European Committee for Standardization (CEN), 2007, Brussels, Belgium, 30 pp.

3 NFPA 68, *Standard on explosion protection by deflagration venting*, National Fire Protection Association (NFPA), 2013, Quincy, Massachusetts, USA.

4 Sommersel, O.K., Bjerketvedt, D, Christensen, S., Krest, O. & Vaagsaether, K., Application of background oriented Schlieren for quantitative measurements of shock waves from explosions, *Shock Waves*, **18**, 2008, pp. 291-297.

5 Sommersel, O.K., Vaagsaether, K. & Bjerketvedt, D., Hydrogen explosions in 20′ ISO container. *International Journal of Hydrogen Energy*, **42**, 2017, pp. 7740-7748.

6 Skjold, T., Lakshmipathy, S., van Wingerden, M., Hisken, H., Atanga, G., Olsen, K.L., Holme, M.N., Turøy, N.M., Mykleby, M & van Wingerden, K., Experimental investigation of vented hydrogen deflagrations in containers – Phase 1: Homogeneous mixtures, 2017, Report HySEA-D2-04-2017.

7 Skjold, T., Hisken, H., Lakshmipathy, S., Atanga, G., van Wingerden, M., Olsen, K.L., Holme, M.N., Turøy, N.M., Mykleby, M & van Wingerden, K., Influence of congestion on vented hydrogen deflagrations in 20-foot ISO containers: homogeneous fuel-air mixtures, Twenty-Sixth International Colloquium on the Dynamics of Explosions and Reactive Systems (ICDERS), Boston, 30 July – 4 August 2017, 6 pp.

8 Savitzky, A. & Golay, J.E., Smoothing and differentiation of data by simplified least squares, *Analytical Chemistry*, **36**, 1964, pp. 1627-1639.

9 Holtappels, K., *Report on the experimentally determined explosion limits, explosion pressures and rates of explosion pressure rise, Part 1: methane, hydrogen and propylene*, SAFEKINEX Project Deliverable No. 8, 2006), Federal Institute for Materials Research and Testing (BAM), Germany, 149 pp.